The Rac-GAP Bcr is a novel regulator of the Par complex that controls cell polarity

Anjana S. Narayanan[a], Steve B. Reyes[b], Kyongmi Um[c], Joseph H. McCarty[b], and Kimberley F. Tolias[a,c]

[a]Verna and Marrs McLean Department of Biochemistry and Molecular Biology and [c]Department of Neuroscience, Baylor College of Medicine, Houston, TX 77030; [b]Department of Cancer Biology, University of Texas M.D. Anderson Cancer Center, Houston, TX 77030

ABSTRACT **Cell polarization is essential for many biological processes, including directed cell migration, and loss of polarity contributes to pathological conditions such as cancer. The Par complex (Par3, Par6, and PKCζ) controls cell polarity in part by recruiting the Rac-specific guanine nucleotide exchange factor T-lymphoma invasion and metastasis 1 (Tiam1) to specialized cellular sites, where Tiam1 promotes local Rac1 activation and cytoskeletal remodeling. However, the mechanisms that restrict Par-Tiam1 complex activity to the leading edge to maintain cell polarity during migration remain unclear. We identify the Rac-specific GTPase-activating protein (GAP) breakpoint cluster region protein (Bcr) as a novel regulator of the Par-Tiam1 complex. We show that Bcr interacts with members of the Par complex and inhibits both Rac1 and PKCζ signaling. Loss of Bcr results in faster, more random migration and striking polarity defects in astrocytes. These polarity defects are rescued by reducing PKCζ activity or by expressing full-length Bcr, but not an N-terminal deletion mutant or the homologous Rac-GAP, Abr, both of which fail to associate with the Par complex. These results demonstrate that Bcr is an integral member of the Par-Tiam1 complex that controls polarized cell migration by locally restricting both Rac1 and PKCζ function.**

Monitoring Editor
Carole Parent
National Institutes of Health

Received: Jun 20, 2013
Revised: Oct 10, 2013
Accepted: Oct 16, 2013

INTRODUCTION

Directional cell migration is essential for embryonic development, immune surveillance, and wound healing, whereas aberrant migration is associated with developmental disorders, inflammatory diseases, and cancer (Ridley, 2001; Etienne-Manneville and Hall, 2002; Aranda *et al.*, 2008; Iden and Collard, 2008; Ellenbroek *et al.*, 2012a). To migrate in a persistent directional manner, cells must establish and maintain polarity with defined leading and trailing edges. Rho-family small GTPases play essential roles in controlling front–rear polarity during cell migration by regulating cytoskeletal dynamics (Ridley, 2001; Etienne-Manneville and Hall, 2002). In general, Rac1 and Cdc42 promote protrusive activity at the leading edge by stimulating actin and microtubule rearrangements, whereas RhoA induces actomyosin contractility and retraction at the trailing edge (Etienne-Manneville and Hall, 2002). Cdc42 also directly regulates cell orientation during migration in response to extracellular cues (Etienne-Manneville, 2004). Rho GTPases regulate these processes by functioning as molecular switches, cycling between an active GTP-bound state and an inactive GDP-bound state with the aid of guanine nucleotide exchange factors (GEFs) and GTPase-activating proteins (GAPs), respectively (Schmidt and Hall, 2002; Tcherkezian and Lamarche-Vane, 2007).

The evolutionarily conserved Par complex, consisting of Par3, Par6, and atypical PKC (PKCζ), also plays essential roles in guiding cell polarity (Etienne-Manneville and Hall, 2003b; Mertens *et al.*, 2006). In migrating cells, activation of the Par complex at the leading edge reorients the centrosome (microtubule-organizing center),

This article was published online ahead of print in MBoC in Press (http://www.molbiolcell.org/cgi/doi/10.1091/mbc.E13-06-0333) on October 23, 2013.

A.S.N. and K.F.T. designed and analyzed the experiments presented in this study. A.S.N. and K.U. made the constructs used, except where noted. S.B.R. helped image and analyze the scratch assay and random migration movies. All other experiments were performed and analyzed by A.S.N. A.S.N. performed all statistical analyses and assembled all of the figures. A.S.N. and K.F.T. wrote the paper.

Address correspondence to: Kimberley F. Tolias (tolias@bcm.edu).

Abbreviations used: Abr, active Bcr-related protein; Bcr, breakpoint cluster region protein; CFP, cyan fluorescent protein; DIV, days in vitro; DMSO, dimethyl sulfoxide; DTT, dithiothreitol; GAP, GTPase-activating protein; GEF, guanine nucleotide exchange factor; GSK-3β, glycogen synthase kinase-3β; GST, glutathione *S*-transferase; HBSS, Hank's balanced salt solution; IgG, immunoglobulin G; PAK, p21-activated kinase; PBD, p21-binding domain; PBS, phosphate-buffered saline; Tiam1, T-lymphoma invasion and metastasis 1; WT, wild type.

microtubule cytoskeleton, and membrane traffic toward the direction of migration (Etienne-Manneville and Hall, 2003b). It has become increasingly clear that cell polarization requires extensive cross-talk between the Par complex and Rho GTPases (Iden and Collard, 2008). For example, activated Cdc42 binds to Par6 and promotes localized PKCζ activity, which in turn modulates microtubule organization and cell orientation (Etienne-Manneville and Hall, 2001; Nishimura *et al.*, 2005). Furthermore, Par3 recruits the Rac-GEF T-lymphoma invasion and metastasis 1 (Tiam1) to specialized sites, where Tiam1 activates Rac1, resulting in local actin polymerization and microtubule stabilization (Nishimura *et al.*, 2005; Zhang and Macara, 2006). To properly control cell polarity, the activities of Rho GTPases and Par-complex proteins must be spatially and temporally regulated, and loss of this tight regulation can result in pathological conditions such as cancer (Eder *et al.*, 2005; Regala *et al.*, 2005a; Iden and Collard, 2008; Rathinam *et al.*, 2011; Ellenbroek *et al.*, 2012a; Mardilovich *et al.*, 2012). However, little is known about the mechanisms that restrict Rho GTPase and Par-complex function at the leading edge to maintain cell polarity during directional cell migration. In this paper, we report the identification of the Rac-GAP breakpoint cluster region protein (Bcr) as a novel regulator of the Par-Tiam1 polarity complex. We show that Bcr interacts with members of the Par complex and that loss of Bcr results in elevated Rac1 activity and consequently enhanced PKCζ signaling in primary astrocytes. Bcr-deficient astrocytes migrate randomly and exhibit polarity defects, in contrast to wild-type (WT) astrocytes and astrocytes lacking the highly related Rac-GAP active Bcr-related protein (Abr). These polarity defects are rescued by reducing PKCζ activity or by expressing full-length Bcr, but not Abr or an N-terminal deletion mutant of Bcr, both of which fail to associate with the Par-Tiam1 complex. Together these results suggest that Bcr is an essential regulator of the Par-Tiam1 complex that controls polarized migration by locally restricting Rac1 and PKCζ function at the leading edge.

RESULTS

Loss of the Rac-GAP Bcr results in increased Rac1 signaling and faster migration in astrocytes

Recently we identified Bcr as Tiam1-interacting protein (unpublished data). While Bcr is best known for its involvement in a chromosomal translocation that causes chronic myelogenous leukemia (Groffen and Heisterkamp, 1997), native Bcr and the closely related protein Abr function in vivo as Rac-GAPs (Cho *et al.*, 2007). We hypothesized that Bcr and/or Abr may cooperate with Tiam1 to precisely regulate Rac1 signaling during directional cell migration. To investigate this possibility, we examined the roles of Bcr and Abr in astrocytes, which not only play pivotal roles in regulating brain development, function, and cancer, but also serve as a model system for elucidating mechanisms of polarized migration (Etienne-Manneville, 2006). We first determined the effects of loss of Bcr and/or Abr on Rac1 signaling by isolating cortical astrocytes from postnatal WT, $Bcr^{-/-}$, $Abr^{-/-}$ and $Bcr^{-/-}Abr^{-/-}$ mice and culturing them for 14 d in vitro (DIV). Cells were then lysed and subjected to a Rac1 activation assay, which utilizes the p21-binding domain (PBD) of the Rac1 effector p21-activated kinase (PAK) as an affinity reagent to precipitate the active Rac-GTP from cells (Sander *et al.*, 1998). We found that $Abr^{-/-}$, $Bcr^{-/-}$, and $Bcr^{-/-}Abr^{-/-}$ astrocytes all exhibited elevated levels of activated Rac1 compared with WT astrocytes (Figure 1, A and B). Rac-dependent PAK autophosphorylation was also increased in $Abr^{-/-}$, $Bcr^{-/-}$, and $Bcr^{-/-}Abr^{-/-}$ astrocytes relative to WT astrocytes (Figure 1, C and D). These results indicate that Bcr and Abr negatively regulate Rac1 signaling in astrocytes.

Because Rac1 is a key regulator of cell migration, we next determined whether loss of Bcr and/or Abr affects astrocyte migration. Astrocyte migration was stimulated using an in vitro wound-healing assay, in which a monolayer of astrocytes is scratched to trigger polarized migration perpendicular to the wound (Etienne-Manneville, 2006). We found that $Bcr^{-/-}$ and $Bcr^{-/-}Abr^{-/-}$ astrocytes closed the wound significantly faster than WT or $Abr^{-/-}$ cells (Figure 1, E and F, and Supplemental Movies S1–S4). This enhanced wound healing could be caused by increased cell proliferation and/or motility. However, bromodeoxyuridine (BrdU) labeling revealed no significant difference between WT and mutant astrocytes, indicating that the astrocytes proliferate at the same rate (Figure S1). To determine whether loss of Bcr and/or Abr directly affects cell motility, we measured nuclear displacement. Bcr-deficient astrocytes moved a greater distance over a 24-h period than WT or $Abr^{-/-}$ cells, suggesting Bcr normally reduces cell speed (Figure 1G). This increased speed observed in astrocytes lacking Bcr was due to elevated Rac1 activity, because NSC23766, a small-molecule inhibitor that specifically blocks Rac1 activation by the Rac-GEFs Tiam1 and Trio (Gao *et al.*, 2004), slowed the rate of wound closure in $Bcr^{-/-}$ and $Bcr^{-/-}Abr^{-/-}$ astrocytes to WT levels (Figure 1H). Thus these results suggest that by inhibiting Rac1, Bcr normally restricts the speed of cell migration.

Bcr deficiency impairs persistent polarized migration in astrocytes

To determine whether Bcr also controls the directionality of cell motility, we performed time-lapse imaging on WT and mutant astrocytes during wound healing, tracking their paths over a 48-h time period (Etienne-Manneville, 2006; Supplemental Movies S1–S4). In contrast to WT and $Abr^{-/-}$ astrocytes, which migrated in a relatively straight line perpendicular to the scratch, $Bcr^{-/-}$ and $Bcr^{-/-}Abr^{-/-}$ astrocytes migrated in more random, less persistent paths (Figure 2A). Bcr-deficient astrocytes plated at low density also displayed more random migration over a 15-h time period than did WT or $Abr^{-/-}$ astrocytes (Figure 2B and Supplemental Movies S5–S8). These effects were quantified using the ratio of the direct linear distance (*D*) to the total distance (*T*) traversed by the cell. Bcr-deficient astrocytes exhibited an approximate 2.6-fold decrease in their *D*:*T* directionality ratio compared with WT or $Abr^{-/-}$ astrocytes (Figure 2C), suggesting that Bcr normally helps to define the direction of migration.

In wound-healing assays, astrocytes typically become polarized prior to migrating and closing the wound (Etienne-Manneville, 2006). This polarization involves the formation of an elongated protrusion toward the scratch, extension of microtubules that permeate the protrusion, and a reorientation of the centrosome toward the direction of migration (Etienne-Manneville, 2006). Because Bcr-deficient astrocytes exhibit decreased directional migration, we tested whether they polarize correctly in the wound-healing assay. To assess protrusion formation and microtubule network polarization, we stained WT and mutant astrocytes with acetylated tubulin to visualize microtubules and with Hoechst to mark nuclei. Following wounding, ~61% of WT and 57% of $Abr^{-/-}$ astrocytes formed polarized protrusions in the direction of the scratch, while only 34% of $Bcr^{-/-}$ and 29% of $Bcr^{-/-}Abr^{-/-}$ astrocytes did (Figures 2, D and E, and S2A). Furthermore, WT and $Abr^{-/-}$ astrocytes displayed properly oriented and organized microtubule and actin cytoskeletons, whereas microtubules and actin filaments in $Bcr^{-/-}$ and $Bcr^{-/-}Abr^{-/-}$ astrocytes were highly disorganized (Figures 2D and S2, B and C). To assess centrosome reorientation, we stained astrocytes with α-pericentrin antibodies to mark centrosomes and Hoechst to mark nuclei at 0 or 18 h after scratching. Normally, in response to wounding, the centrosome of each cell will move from a random location around the nucleus to

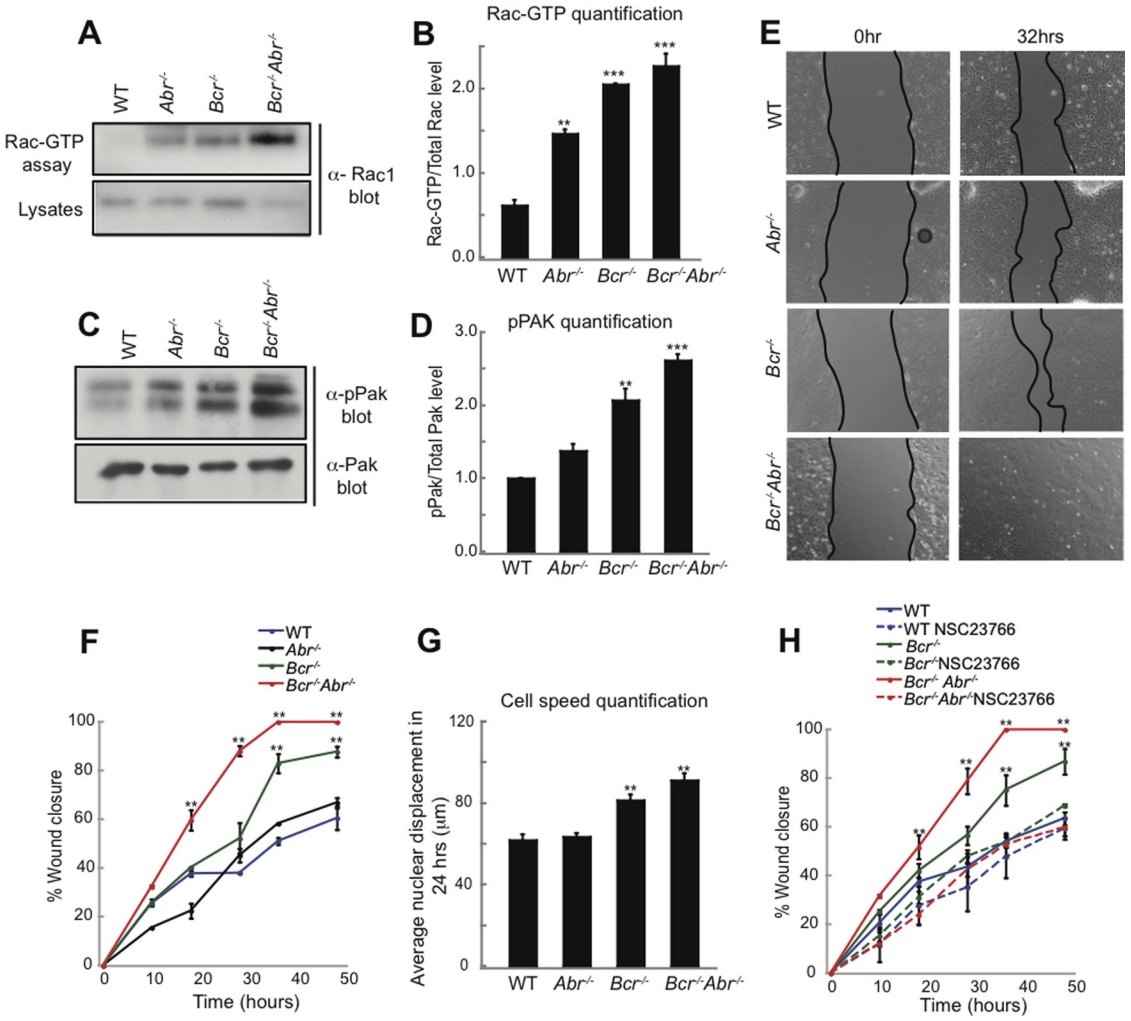

FIGURE 1: Bcr loss results in increased Rac1 signaling and faster migration in astrocytes. (A) Western blot analysis of the Rac1 activation assay. Activated Rac1 was affinity-purified from WT, *Abr*$^{-/-}$, *Bcr*$^{-/-}$, and *Bcr*$^{-/-}$ *Abr*$^{-/-}$ cortical astrocyte lysates using GST-PBD, and then immunoblotted with α-Rac1 antibodies. Total lysates were also probed for Rac1 to show protein loading. Mutant astrocytes displayed elevated levels of activated Rac1 relative to WT astrocytes. (B) Quantification of Rac1 activation assay. $N = 3$. (C) Western blot analysis of Pak phosphorylation (pPak). Total levels of Pak are also shown. Loss of the Rac-GAPs Bcr and/or Abr results in increased Pak phosphorylation in cortical astrocytes. (D) Quantification of Pak phosphorylation. $N = 3$. (E) Representative images of a scratch assay performed on mouse cortical astrocytes. Astrocytes from WT, *Abr*$^{-/-}$, *Bcr*$^{-/-}$, and *Bcr*$^{-/-}$*Abr*$^{-/-}$ mice were scratched and imaged over a time period of 48 h. *Bcr*$^{-/-}$ and *Bcr*$^{-/-}$*Abr*$^{-/-}$ astrocytes closed the wound faster than WT or *Abr*$^{-/-}$ astrocytes, as shown by the representative images at the 32-h time point. (F) Quantification of the scratch assays. Percentage of wound closure was quantified over 48 h in scratch assays performed on WT, *Abr*$^{-/-}$, *Bcr*$^{-/-}$, and *Bcr*$^{-/-}$*Abr*$^{-/-}$ astrocytes. $N = 4$. (G) Quantification of cell speed. Nuclear displacements of WT, *Abr*$^{-/-}$, *Bcr*$^{-/-}$, and *Bcr*$^{-/-}$*Abr*$^{-/-}$ astrocytes were measured over 24 h during the scratch assay. $N = 3$. (H) Quantification of scratch assays done in the absence or presence of the Tiam1-Rac1 small-molecule inhibitor NSC23766. Percentage of wound closure was quantified over 48 h in scratch assays performed on WT, *Abr*$^{-/-}$, *Bcr*$^{-/-}$, and *Bcr*$^{-/-}$*Abr*$^{-/-}$ astrocytes treated with PBS (control) or 50 μM NSC23766. Treatment with NSC23766 slowed down Bcr-deficient astroctyes to WT levels. $N = 4$. Data are shown ± SEM.

the front of the nucleus in the quadrant facing the scratch (scored as a polarized centrosome; see Figure 2F; Etienne-Manneville, 2006). We found that, after wounding, ~75% of WT and *Abr*$^{-/-}$ astrocytes possessed polarized centrosomes, whereas polarized centrosomes were present in only 27% of *Bcr*$^{-/-}$ and *Bcr*$^{-/-}$*Abr*$^{-/-}$ astrocytes (Figure 2, G and H). Because 27% is not different from chance orientation, this result suggests that Bcr-deficient astrocytes fail to reorient their centrosomes toward the scratch. Together these results indicate that Bcr plays an important role in the establishment of cell polarization in addition to the regulation of cell speed.

Bcr is a novel member of the Par-Tiam1 complex

How might Bcr regulate cell polarization? As previously noted, we recently discovered that Bcr interacts with the Rac-GEF Tiam1 (unpublished data), a key component of the Par complex (Mertens *et al.*, 2006; Nakayama *et al.*, 2008). During directional migration, Tiam1 promotes Rac-dependent protrusion formation at the leading edge by inducing actin polymerization and microtubule stabilization (Pegtel *et al.*, 2007; Ellenbroek *et al.*, 2012b), while Par6-PKCζ controls centrosome reorientation by phosphorylating and inactivating glycogen synthase kinase-3β (GSK-3β; Etienne-Manneville and

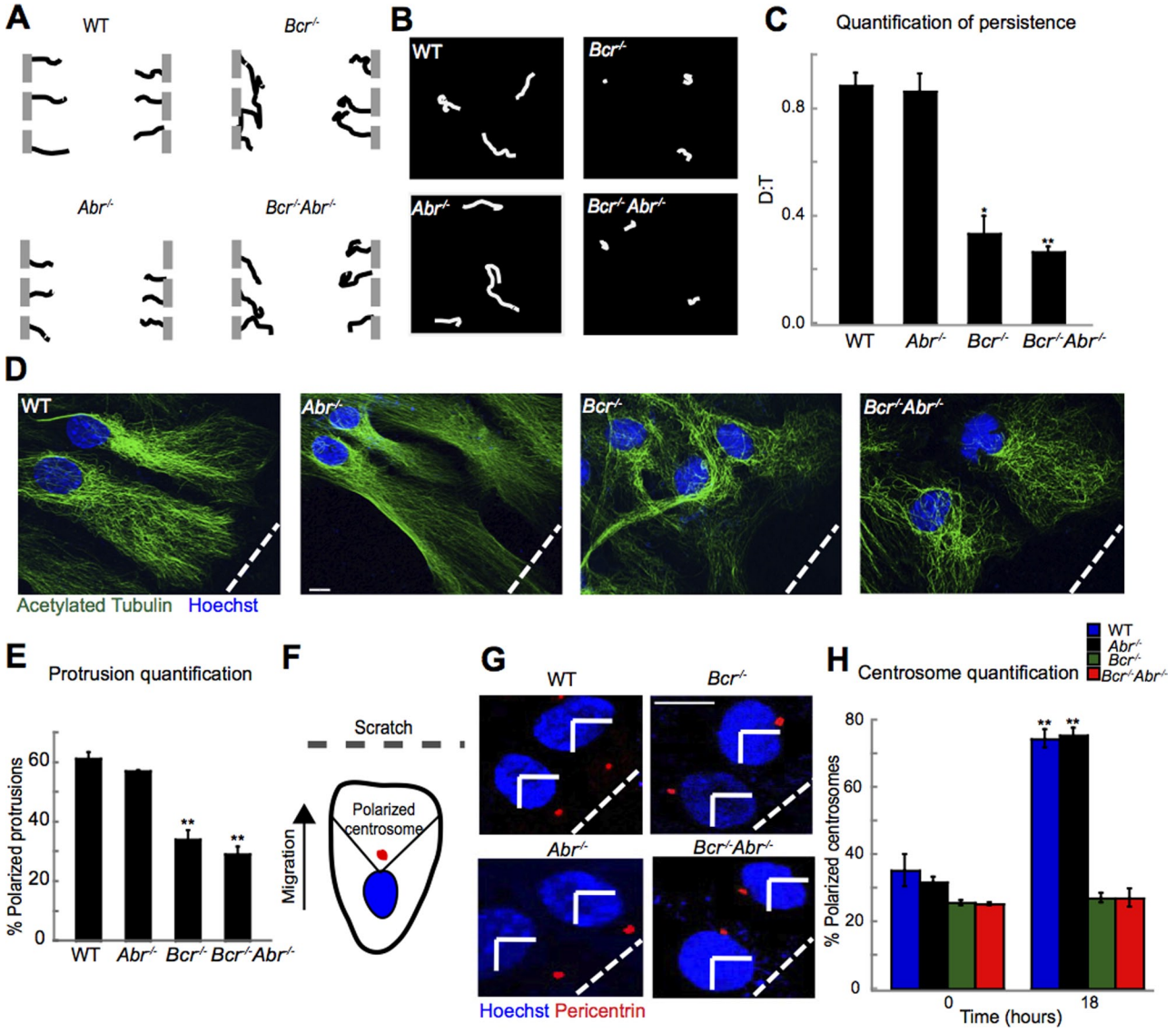

FIGURE 2: Loss of Bcr impairs persistent polarized migration in astrocytes. (A) Representative individual migration tracks of WT, *Abr*$^{-/-}$, *Bcr*$^{-/-}$, and *Bcr*$^{-/-}$*Abr*$^{-/-}$ cortical astrocytes from the wound-healing assay. $N = 3$. (B) Representative individual migration tracks of WT *Abr*$^{-/-}$, *Bcr*$^{-/-}$, and *Bcr*$^{-/-}$*Abr*$^{-/-}$ astrocytes plated at low density. $N = 3$. (C) Quantification of average persistence (*D*:*T* ratio) of migrating WT, *Abr*$^{-/-}$, *Bcr*$^{-/-}$, and *Bcr*$^{-/-}$*Abr*$^{-/-}$ astrocytes derived from the tracks depicted in (B). A persistence of 1 indicates completely linear migration. $N = 3$. (D) Protrusion assay. WT, *Abr*$^{-/-}$, *Bcr*$^{-/-}$, and *Bcr*$^{-/-}$*Abr*$^{-/-}$ astrocyte monolayers were scratched at time 0, and then fixed 18 h postscratch and stained with α-acetylated tubulin antibodies to mark microtubules (green) and Hoechst to mark nuclei (blue). WT and *Abr*$^{-/-}$ astrocytes formed polarized protrusions perpendicular to the scratch (indicated by the white dashed line), while *Bcr*$^{-/-}$ and *Bcr*$^{-/-}$*Abr*$^{-/-}$ astrocytes failed to form polarized protrusions. Scale bar: 10 μm. (E) Quantification of the protrusion assay shown as percent of cells with polarized protrusions. $n = \sim100$; $N = 3$. (F) Centrosome reorientation assay. Cortical astrocytes were scratched and fixed at 0 and 18 h postscratch and stained with Hoechst (nuclei: blue) and α-pericentrin antibodies (centrosomes: red). Cells with centrosomes in the front marked quadrant were quantified as having polarized centrosomes. (G) Representative images of centrosome reorientation assay. By 18 h, most WT and *Abr*$^{-/-}$ astrocytes possessed correctly polarized centrosomes, while *Bcr*$^{-/-}$ and *Bcr*$^{-/-}$*Abr*$^{-/-}$ astrocytes failed to reorient their centrosomes in the polarized direction. Scale bar: 5 μm. (H) Quantification of the centrosome reorientation assay. $N = 3$. Data are shown ± SEM.

Hall, 2003a; Figure 3A). Because Bcr is required for both protrusion formation and centrosome reorientation (Figure 2, D–H), we hypothesized that Bcr may associate with the Par-Tiam1 complex and restrict Rac1 and PKCζ activity at the leading edge. To investigate this possibility, we first tested whether Bcr interacts with members of the Par complex. COS7 cells were transfected with expression plasmids encoding Par3 alone or in combination with Flag-tagged Bcr or Tiam1 (as a positive control), and then Bcr or Tiam1 was immunoprecipitated with an anti-Flag antibody. As shown in Figure 3B, Par3 coimmunoprecipitated with both Bcr and Tiam1, but not with control anti-Flag immunoprecipitates. Par3 was also present in Bcr immunoprecipitates from rat cortical astrocyte cultures (Figure 3C),

suggesting that endogenous Bcr and Par3 interact. We performed similar experiments to assess the association between Bcr and PKCζ. We found that Bcr and PKCζ coimmunoprecipitate from both COS7 cells (Figure 3D) and primary rat cortical astrocytes (Figure 3E). These results suggest that, like Tiam1, Bcr interacts with both PKCζ and Par3. In contrast, we detected no interaction between Par6 and either Bcr or Tiam1 when Par6 was overexpressed alone with these proteins in COS7 cells (Figure S3A). However, when Par6 was coexpressed with Tiam1 or Bcr in the presence of PKCζ, Par6 coimmunoprecipitated with both Tiam1 and Bcr, suggesting that PKCζ facilitates their interaction with Par6 (Figure 3F). From these results, we conclude that Bcr is a novel member of the Par complex with an interaction profile similar to that of Tiam1, a well-defined polarity complex member. Interestingly, in contrast to Bcr, the homologous Rac-GAP Abr did not associate with any members of the Par complex (Figure S3, B and C), consistent with its lack of involvement in astrocyte polarization (Figure 2, D–H).

To determine which domain(s) of Bcr mediate its interaction with the Par complex, we generated glutathione *S*-transferase (GST)-tagged fusion proteins containing different regions of Bcr, including the DH-PH (GEF) domain, the GAP domain, and the N-terminal serine/threonine protein kinase domain with (N-term) or without (N-termΔO) the oligomerization domain (Figure 3G). These GST-fusion proteins were immobilized on glutathione beads and then used to pull down Par3 or PKCζ overexpressed in HEK293T cells. We found that Par3 interacted with the GEF, GAP, and oligomerization-containing N-terminal (N-term) Bcr constructs, whereas PKCζ associated only with Bcr constructs containing the N-terminus (N-term and N-termΔO) (Figure 3, G and H). The N-terminus of Bcr also mediates its interaction with Tiam1 (unpublished data). Interestingly, Abr, which fails to interact with Par-complex members (Figure S3, B and C), lacks an equivalent N-terminal oligomerization and kinase domain (Figure 3G), suggesting that this region of Bcr is important for its association with the Par-Tiam1 complex. To confirm this possibility, we made an N-terminal deletion construct of Bcr (ΔN-Bcr) and found that, similar to Abr, ΔN-Bcr does not associate with PKCζ (Figure 3, G and I).

The Par-Tiam1 complex functions at the leading edge to control directional cell migration (Etienne-Manneville and Hall, 2001; Cau and Hall, 2005; Gomes *et al.*, 2005; Pegtel *et al.*, 2007; Nakayama *et al.*, 2008). Because Bcr interacts with members of the Par-Tiam1 complex, it may also be recruited to the leading edge during cell migration. To test this possibility, we performed a scratch assay on rat cortical astrocytes expressing low levels of cyan fluorescent protein (CFP)-tagged Bcr. Prior to wounding, Bcr was localized diffusely throughout the cell, but by 18 h postscratch, Bcr was clearly enriched at the plasma membrane of the leading edge (Figure 3J). We also found that Bcr colocalized with PKCζ at the leading edge of migrating astrocytes (Figure 3K). In contrast to its localization, Bcr's interaction with Par-complex members did not appear to be dramatically altered following wounding in the scratch assay (Figure S3, D and E). Together these results suggest that, in response to a promigratory stimulus, Bcr and Par-complex members translocate together to the leading edge, where they control directed cell migration.

Bcr negatively regulates PKCζ signaling by facilitating its degradation

Because Bcr interacts with PKCζ (Figure 3, D and E) and is required for aspects of cell polarization known to be regulated by PKCζ (Figure 2, G and H), we hypothesized that Bcr may play an important role in PKCζ signaling. Consistent with our hypothesis, Western blot analyses of lysates obtained from WT and *Bcr*$^{-/-}$ astrocytes revealed that PKCζ levels were significantly greater in *Bcr*$^{-/-}$ astrocytes compared with WT astrocytes (Figure 4, A and B), suggesting that Bcr normally down-regulates PKCζ levels. Furthermore, immunostaining studies performed on astrocytes migrating in a wound-healing assay showed that PKCζ was more abundant and less confined to the leading-edge plasma membrane in *Bcr*$^{-/-}$ astrocytes than in WT astrocytes (Figure 4C). In contrast, Par3 and Tiam1 localization was unaffected by the absence of Bcr (Figure S4, A and B). PKCζ is known to phosphorylate GSK-3β on Ser-9, which inhibits the catalytic activity of GSK-3β and suppresses its ability to phosphorylate and target β-catenin for ubiquitination and proteasomal degradation (Li *et al.*, 1999; Moon *et al.*, 2002). To determine whether the increased PKCζ levels observed in Bcr-deficient astrocytes result in enhanced PKCζ signaling, we examined GSK-3β phosphorylation and β-catenin levels in WT and *Bcr*$^{-/-}$ astrocytes. We found that *Bcr*$^{-/-}$ astrocytes exhibited an increase in both GSK-3β phosphorylation (Figure 4, D and E) and β-catenin stabilization (Figure 4, F and G) relative to WT astrocytes. This enhanced GSK3β phosphorylation was confirmed to be PKCζ-dependent, because treatment of *Bcr*$^{-/-}$ astrocytes with a myristoylated PKCζ pseudosubstrate inhibitor reduced GSK3β phosphorylation to WT levels (Figure S4, C and D). These results demonstrate that Bcr inhibits PKCζ downstream signaling. In contrast, we did not detect any alterations in PKCζ or phospho–GSK-3β levels in Abr$^{-/-}$ astrocytes (Figure S4, E–G). Thus these results suggest that Bcr regulates cell polarity not only by limiting Rac1 activation but also by down-regulating PKCζ levels and function.

Because PKCζ levels are high in the absence of Bcr (Figure 4, A–C) and PKCζ is a known target of the ubiquitin-proteasome pathway (Smith *et al.*, 2000), we next asked whether Bcr negatively regulates PKCζ signaling by facilitating its degradation. To investigate this possibility, we overexpressed myc-Bcr or control vector in COS7 cells, treated the cells with vehicle (dimethyl sulfoxide [DMSO]) or MG132 for 6 h to inhibit proteasome-dependent degradation, and then analyzed endogenous PKCζ levels by Western blotting with an anti–PKCζ antibody. We found that Bcr overexpression significantly reduced PKCζ levels relative to control levels (Figure 4, H and I). However, treatment with the proteasome inhibitor MG132 prevented this Bcr-induced PKCζ decrease (Figure 4, H and I), suggesting that Bcr promotes PKCζ degradation.

Activated Rac1 and Cdc42 are both capable of forming a ternary complex with Par6 and PKCζ, resulting in increased PKCζ stability and kinase activity (Qiu *et al.*, 2000). Because Bcr negatively regulates Rac1, we examined whether the ability of Bcr to promote PKCζ degradation is Rac-dependent. While Bcr caused a significant reduction in PKCζ levels when overexpressed in COS7 cells (Figure 4, J and K), a Bcr mutant that lacks Rac-GAP activity (Bcr-GD) failed to lower PKCζ levels below control levels (Figure 4, J and K). Furthermore, the effect of Bcr on PKCζ was blocked by coexpression with a constitutively active Rac1 mutant (RacV12; Figure 4, J and K). These results suggest that Bcr induces PKCζ degradation by inhibiting Rac1 activity. To confirm that Bcr regulates PKCζ degradation in astrocytes in a Rac-dependent manner, we treated WT and *Bcr*$^{-/-}$ astrocytes with NSC23766 to inhibit Tiam1-mediated Rac1 activation, which is elevated in Bcr-deficient astrocytes (Figure 1, A and B). In the absence of NSC23766, *Bcr*$^{-/-}$ astrocytes displayed increased levels of PKCζ compared with levels in WT (Figure 4, L and M). However, treatment with NSC23766 reduced PKCζ levels in *Bcr*$^{-/-}$ astrocytes to WT levels (Figure 4, L and M). Because activated Cdc42 levels are not elevated in *Bcr*$^{-/-}$ astrocytes (Figure S4, H and I), these findings indicate that Bcr promotes PKCζ degradation by inhibiting Rac1 activity.

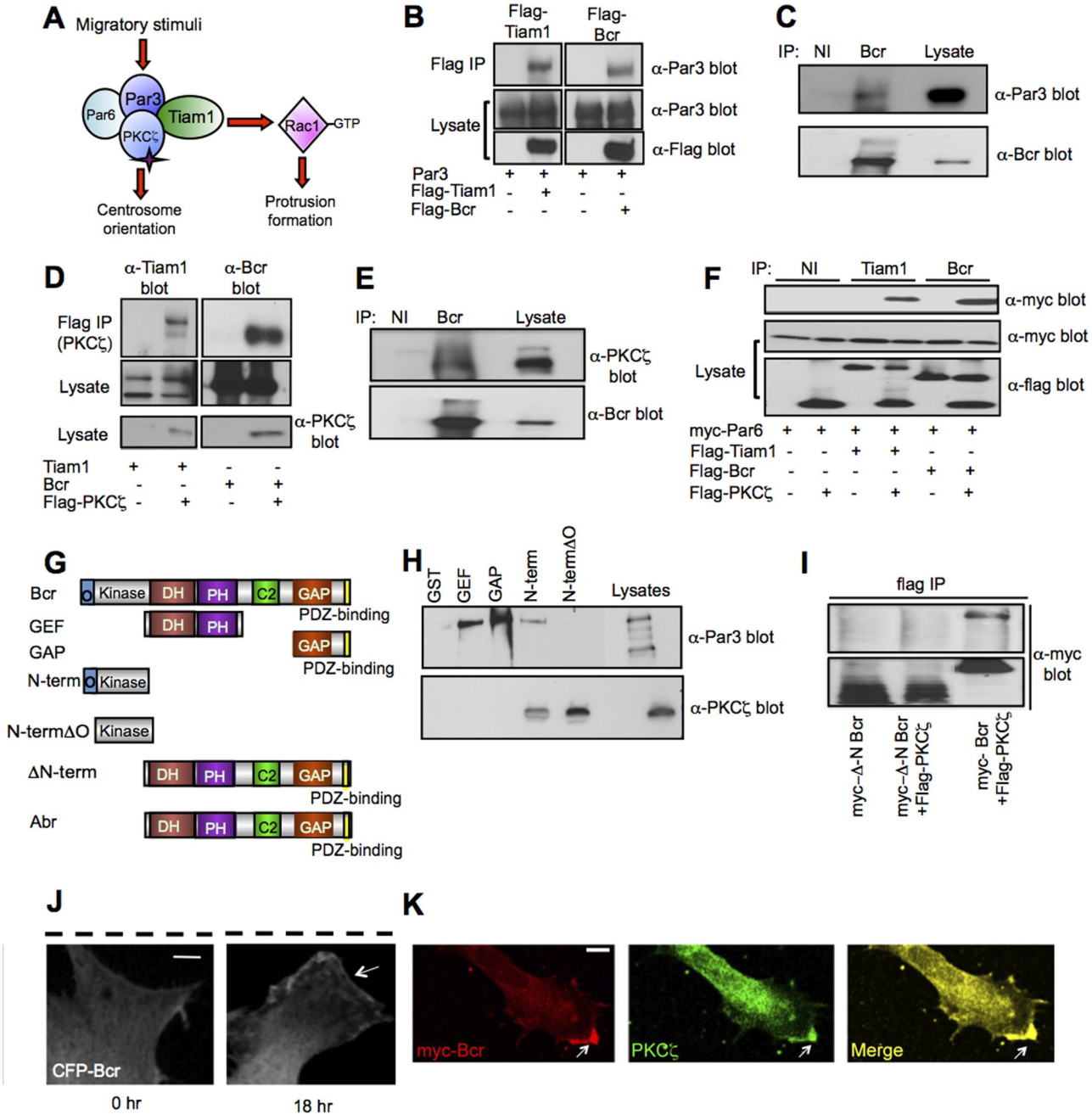

FIGURE 3: Bcr is a novel interaction partner of the Par-Tiam1 complex. (A) Schematic depicting the role of the Par-Tiam1 complex in polarized cell migration. Tiam1-mediated Rac1 activation promotes cytoskeletal remodeling important for protrusion formation, whereas PKCζ regulates the reorientation of the centrosome. (B) Bcr interacts with Par3 in COS7 cells. Lysates from COS7 cells expressing Par3 in the presence or absence of Flag-tagged Bcr or Tiam1 (positive control) were immunoprecipitated (IP) with an α-Flag antibody, and then immunoblotted with an α-Par3 antibody. Lysates were also immunoblotted with α-Par3 and α-Flag antibodies to demonstrate protein expression. *N* = 3. (C) Bcr interacts with Par3 in astrocytes. Lysates from cultured rat cortical astrocytes (DIV21) were immunoprecipitated with control immunoglobulin G (IgG; nonimmune: NI) or α-Bcr antibodies, and then immunoblotted with the α-Par3 or α-Bcr antibody. *N* = 3. (D) Bcr interacts with PKCζ in COS7 cells. Lysates from COS7 cells expressing Tiam1 (positive control) or Bcr alone or in combination with Flag-PKCζ were immunoprecipitated with α-Flag antibody, and then immunoblotted with α-Tiam1 or α-Bcr antibodies. Lysates were also blotted with α-Tiam1, α-Bcr, or α-Flag antibodies to confirm protein expression. *N* = 3. (E) Bcr interacts with PKCζ in cortical astrocytes. Lysates from cultured rat cortical astrocytes (DIV21) were immunoprecipitated with control IgG (NI) or α-Bcr antibodies, and then immunoblotted with α-PKCζ or α-Bcr antibodies. *N* = 3. (F) Bcr and Tiam1 require PKCζ to interact with Par6 in COS7 cells. Flag-tagged Tiam1 or Bcr was coexpressed alone or in combination with myc-Par6 in the absence or presence of Flag-PKCζ. Tiam1 and Bcr were immunoprecipitated with α-Tiam1 or α-Bcr antibodies, respectively, and then immunoblotted with anti-myc antibody to assess Par6 association. Lysates were blotted with α-Flag antibody to confirm protein expression. *N* = 3. (G) Domain structures of full-length Bcr and Abr as well as truncated Bcr constructs used in

Bcr restricts PKCζ function to maintain cell polarity

To investigate whether Bcr's ability to inhibit PKCζ signaling is important for its effects on cell polarity, we subjected WT and *Bcr*$^{-/-}$ astrocytes to the wound-healing assay in the presence or absence of a myristoylated PKCζ pseudosubstrate inhibitor. Astrocytes were then imaged and analyzed for protrusion formation and centrosome reorientation 18 h following the scratch. Consistent with our previous results, we found that *Bcr*$^{-/-}$ astrocytes displayed defects in both protrusion formation and centrosome reorientation (Figure 5, A and B). Treatment with a low dose of the PKCζ inhibitor that did not disrupt WT astrocyte polarity (Figure 5, A and B) partially rescued the protrusion and centrosome polarity defects in the *Bcr*$^{-/-}$ astrocytes (Figure 5, A and B), indicating that elevated PKCζ activity contributes to the polarity defects observed in *Bcr*$^{-/-}$ astrocytes. This result suggests that Bcr normally controls cell polarity in part by restricting PKCζ activity. The absence of a full rescue may be due to the fact that PKCζ requires precise spatiotemporal regulation to mediate cell polarity (Etienne-Manneville and Hall, 2001) and global inhibition of PKCζ does not fully replicate WT conditions.

We next investigated whether Bcr's ability to interact with the Par complex is important for its capacity to control cell polarity. In contrast to Bcr, Abr is not required for astrocyte cell polarity (Figure 2, D and F) and does not associate with the Par-Tiam1 complex (Figure S3, B and C) or inhibit PKCζ levels (Figure 5, C and D), despite having equivalent Rac-GAP activity (Figure 5, E and F). Consistent with these differences, we found that Bcr, but not Abr, was capable of rescuing the polarity defects observed in *Bcr*$^{-/-}$ astrocytes (Figure 5, G–I). Specifically, *Bcr*$^{-/-}$ astrocytes expressing eGFP and myc-Bcr formed polarized protrusions (Figure 5, G and H) and reoriented their centrosomes toward the scratch (Figure 5I) in a wound-healing assay in a similar manner as eGFP-expressing WT astrocytes, whereas *Bcr*$^{-/-}$ astrocytes expressing eGFP alone or with myc-Abr failed to properly polarize (Figure 5, G–I). Likewise, the ΔN-Bcr mutant, which has equivalent Rac-GAP activity (Figure S5, A and B) but cannot bind to or inhibit PKCζ (Figures 3I and S5, A and C), failed to rescue the polarity defects observed in *Bcr*$^{-/-}$ astrocytes (Figure S5, D and E). Taken together, these results suggest that the ability of Bcr to interact with members of the Par complex and locally restrict Rac1 and PKCζ activity is essential for its regulation of cell polarity.

DISCUSSION

We conclude that Bcr is a novel member of the Par-Tiam1 complex that promotes the proper polarization, orientation, and migration of astrocytes by restricting the levels of active Rac1 and PKCζ. In the absence of Bcr, excessive Rac1 activity results in faster, more random migration; enhanced PKCζ signaling; and defects in the ability of astrocytes to polarize their protrusions and centrosomes toward the direction of migration. These polarity defects can be rescued by reducing PKCζ activity or by reexpressing Bcr. In contrast, the polarity defects cannot be rescued by expressing the highly homologous Rac-GAP Abr or an N-terminally deleted Bcr mutant, which possess equivalent Rac-GAP activities but do not associate with the Par-Tiam1 complex or suppress PKCζ levels. While Bcr and Abr both appear to function as Rac-GAPs in astrocytes, our results indicate that Bcr serves a unique role in regulating cell polarity during migration by interacting with the Par-Tiam1 complex and locally restricting Rac1 and PKCζ function at the leading edge.

Although Bcr-deficient astrocytes lack the ability to move in straight trajectories like WT or Abr$^{-/-}$ astrocytes, they manage to close the wound faster in the scratch assay. This faster wound closure is likely due to the increased cellular velocity of Bcr-deficient astrocytes and the fact that cells in a scratch assay are somewhat restricted in their direction of motion due to contact inhibition from surrounding cells. In contrast to the scratch assay, astrocytes lacking Bcr clearly fail to persistently migrate in the random migration assay, where cells are able to move in any direction. Results from these two migration assays demonstrate that Bcr controls both cell speed and directionality.

While the Rac1 and PKCζ signaling pathways are both required for directed cell migration, they are proposed to serve different roles (Etienne-Manneville and Hall, 2003a). Tiam1-mediated Rac1 signaling promotes protrusion formation at the leading edge by stimulating actin polymerization and microtubule stabilization (Pegtel *et al.*, 2007; Ellenbroek *et al.*, 2012b), whereas Par6-PKCζ signaling controls the reorientation of protrusions and centrosomes toward the direction of migration by regulating GSK-3β signaling (Etienne-Manneville and Hall, 2003a). To properly control directional migration, the activities of both PKCζ and Rac1 need to be precisely regulated. For instance, ectopic activity of Par-complex members, particularly aPKC, can result in loss of polarity and pathological conditions such as tissue disorganization and tumorigenesis (Regala *et al.*, 2005b; Cunliffe *et al.*, 2012). Furthermore, studies analyzing Rac1 activity patterns in migrating cells suggest that Rac1 is also highly spatially and temporally regulated (Kraynov *et al.*, 2000; Gardiner *et al.*, 2002), and disruption of this precise regulation by constitutively active or dominant-negative mutants results in aberrant cell migration (Hooshmand-Rad *et al.*, 1997; Ridley, 2001). However, the mechanisms that restrict Rac1 and PKCζ signaling to maintain cell polarity during migration are not clear. Our results indicate that Bcr serves a novel function in Par-Tiam1 complex–mediated directional migration. Not only does Bcr regulate protrusion formation and cell speed by down-regulating Rac1 activity, it also regulates cell polarity by limiting PKCζ stability and signaling. Bcr may restrict PKCζ signaling to the leading edge by reducing the

the domain-mapping experiments. GEF: Dbl homology and pleckstrin homology (DH-PH) domain; GAP: GTPase-activating protein domain; O: oligomerization domain; Kinase: serine/threonine kinase domain; C2: calcium-dependent lipid-binding domain. (H) The N-terminus of Bcr is important for mediating its interaction with members of the Par complex. Lysates from HEK293T cells expressing full-length Par3 or PKCζ were incubated with recombinant Bcr GST-fusion proteins (GEF, GAP, N-term, and N-termΔO) or GST control protein immobilized on beads. Precipitated proteins were then analyzed by immunoblotting with α-Par3 and α-PKCζ antibodies. $N = 3$. (I) Deletion of the Bcr N-terminus prevents binding of Bcr to PKCζ. Western blot analysis of lysates from COS7 cells transfected with myc-ΔN-Bcr with or without Flag-PKCζ or myc-Bcr and Flag-PKCζ (positive control). Lysates were immunoprecipitated with α-Flag antibody, and then immunoblotted with α-myc antibody. $N = 3$. (J) Representative confocal images showing the localization of CFP-Bcr before and 18 h after wounding in a scratch assay. White arrows point to CFP-Bcr at the leading edge of a polarized migrating astrocyte; the black dashed line indicates the scratch. Scale bar: 10 μm. $n = 20$; $N = 3$. (K) Representative confocal image demonstrating the colocalization of myc-Bcr with endogenous PKCζ at the leading edge of a polarized migrating astrocyte. Scale bar: 10 μm. $n = 20$; $N = 3$.

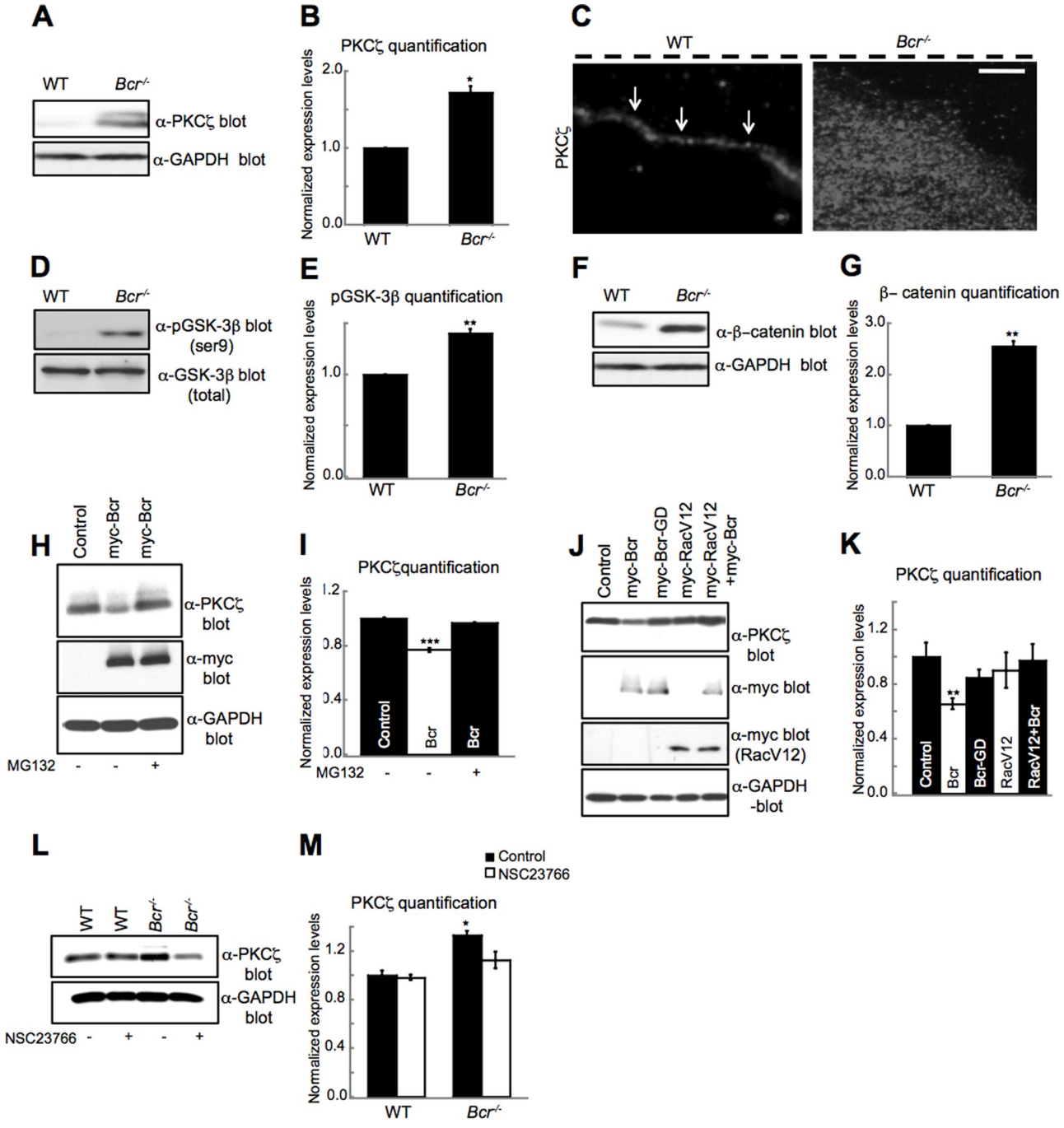

FIGURE 4: Bcr negatively regulates PKCζ signaling by facilitating its degradation. (A) Western blot analysis of lysates obtained from WT and *Bcr*$^{-/-}$ mouse cortical astrocytes. Bcr-deficient astrocytes showed an increase in total PKCζ levels. Lysates were also immunoblotted with α-GAPDH antibodies for a loading control. (B) Quantification of PKCζ levels. $N = 3$. (C) Representative images showing the localization of PKCζ in WT and *Bcr*$^{-/-}$ astrocytes migrating in a scratch assay. PKCζ is localized to the leading edge (white arrows) in WT cells, whereas PKCζ immunostaining was increased and more diffuse in *Bcr*$^{-/-}$ cells. Dashed black line shows scratch location. Scale bar: 10 μm. (D) Western blot analysis of lysates obtained from WT and *Bcr*$^{-/-}$ mouse cortical astrocytes. Bcr-deficient astrocytes showed an increase in p-GSK-3β levels. Lysates were also blotted with total GSK-3β antibodies for a loading control. (E) Quantification of p-GSK-3β levels. $N = 3$. (F) Western blot analysis of lysates obtained from WT and *Bcr*$^{-/-}$ mouse cortical astrocytes. Bcr-deficient astrocytes showed an increase in β-catenin levels. Lysates were also blotted with α-GAPDH antibodies for a loading control. (G) Quantification of β-catenin levels. $N = 3$. (H) Western blot analysis of lysates from COS7 cells expressing myc (control) or myc-Bcr and treated with DMSO (control) or 10 μM of the proteasomal inhibitor MG132. Bcr overexpression reduces PKCζ levels, which is blocked by treating cells with MG132. Lysates were blotted with α-GAPDH antibodies for a loading control. (I) Quantification of PKCζ levels from (H). $N = 3$. (J) The ability of Bcr to reduce PKCζ levels depends on its Rac-GAP activity. Lysates from COS7 cells expressing myc (control) or myc-tagged Bcr, GAP-dead Bcr (BcrGD), constitutively active Rac (RacV12), or RacV12 plus myc-Bcr were immunoblotted with an α-PKCζ antibody. Lysates were

level of active Rac1, preventing it from accumulating and forming a ternary complex with Par6 and PKCζ that stabilizes and enhances PKCζ activity (Qiu *et al.*, 2000). These results indicate that there is more cross-talk between Rac1 and PKCζ signaling pathways than was previously appreciated.

Our results demonstrate that Bcr cooperates with the Par-Tiam1 complex to regulate polarized cell migration in astrocytes. Although astrocytes have traditionally been thought of as neuron support cells, studies now show that astrocytes play a wide range of functions critical for normal brain function and homeostasis (Etienne-Manneville, 2008). For instance, astrocytes respond to CNS insult by undergoing an activation process and migrating to sites of injury, where they form glia scars. Astrocytes also can give rise to malignant astrocytic gliomas, which are the most common and lethal brain tumors in humans. These tumors are particularly fatal, due in large part to their invasive nature. Thus elucidating mechanisms that control astrocyte migration has important implications for promoting CNS regeneration and preventing astrocytic tumor invasion and metastasis.

Bcr also likely cooperates with the Par-Tiam1 complex to regulate other aspects of cell polarity in addition to astrocyte migration. For instance, astrocytes form functional bridges between blood vessels and neurons in the brain to control local blood flow in response to neuronal activity (Etienne-Manneville, 2008). The establishment of this asymmetric cellular interaction may require the functions of Bcr along with the Par-Tiam1 complex. In neurons, Bcr may cooperate with the Par-Tiam1 complex to control myelination (Chan *et al.*, 2006), neuronal migration (Solecki *et al.*, 2006), axon initiation and guidance (Shi *et al.*, 2004; Wolf *et al.*, 2008), and/or synapse formation (Ruiz-Canada *et al.*, 2004; Zhang and Macara, 2006, 2008). Furthermore, outside the nervous system, Bcr may play important roles in other Par-Tiam1 complex–regulated events, such as epithelial tight junction assembly (Chen and Macara, 2005; Mertens *et al.*, 2006). These potential functions of Bcr need to be investigated. Moreover, because the N-terminus of Bcr mediates its interaction with members of the Par-Tiam1 complex, it would be interesting to determine whether the oncogenic fusion protein Bcr-Abl, which contains the N-terminus of Bcr, also affects PKCζ signaling and cellular polarity, and whether this function contributes to its role in chronic myelogenous leukemia.

MATERIALS AND METHODS

DNA constructs

pK-myc-Par3b (plasmid 19388) was obtained from Addgene (Cambridge, MA). Flag-PKCζ was generously provided by Alex Toker (Beth Israel Deaconess Medical Center, Harvard Medical School, Boston, MA). pCMV-myc-Tiam1 and pCMV-myc-RacV12 have been previously described (Tolias *et al.*, 2005, 2007). Full-length human Bcr and Abr and the following truncated Bcr mutants were PCR amplified and subcloned into pCMV-Myc vectors: N-term (oligomerization and serine/threonine kinase domain; aa 1–426), N-termΔO (serine/threonine kinase domain; aa 64–426), GEF (aa 489–866), GAP (aa 1004–1271), and ΔN-Bcr (aa 426–1271). The pCMV-Myc-BcrGD (T1210R) construct was generated using the QuikChange site-directed mutagenesis kit (Stratagene, Agilent, Santa Clara, CA). For the GST pull-down assays, the following regions of Bcr were subcloned into pGEX-4T-2: N-term, N-termΔO, GEF, and GAP. All constructs were verified by DNA sequencing.

Mice

All experiments were done in accordance with procedures approved by the Animal Protocol Review Committee of Baylor College of Medicine according to national and institutional guidelines for animal care established by the National Institutes of Health and approved by a competent animal ethics committee. *Abr*$^{-/-}$ mice were generously provided by Nora Heisterkamp (Children's Hospital Los Angeles, University of Southern California, Los Angeles, CA) and were genotyped using the following primers: forward, GGCCTCAAGAGGGCTAGAGT; reverse WT, CTGTGCTCACCATCCAACAG; and reverse mutant, AGCTCATTCCTCCCACTCATG. *Bcr*$^{-/-}$ mice were obtained from the Jackson Laboratory (Bar Harbor, ME) and genotyped by using the following primers: forward, GAGGAAGAAGGTGAATCATCG; reverse WT, TCATAGCCGAAAGTCCCAAC; and reverse mutant, CCTTCCCGCTTCAGTGCAA. *Abr*$^{-/-}$ and *Bcr*$^{-/-}$ mice were crossed with each other, and *Abr*$^{+/-}$*Bcr*$^{+/-}$ mice were used to generate mice for experiments.

Primary astrocyte culture and transfection

Neonatal brains (P1-3) were removed and placed in sterile, ice-cold Hank's balanced salt solution (HBSS). Whole neocortices were dissected to obtain cortical sheets. The meninges were stripped away, and the cortical sheets were digested for 4 min at 37°C in HBSS containing 20 U/ml papain. The cortical tissue was triturated in DMEM containing 10% calf serum and penicillin/streptomycin. The resulting single-cell suspension was plated onto T-75 tissue culture flasks (~2–3 neonatal brains/flask). After 7–10 d, the astroglial cells formed a confluent monolayer, with neurons, oligodendrocytes, and fibroblasts growing on top. These contaminating cells were removed by rotary shaking the flasks overnight at 250 rpm. The resulting cultures were composed of more than 95% astrocytes, as assessed by anti–glial fibrillary acidic protein (GFAP) immunoreactivity. Immunostaining of cells was performed using standard procedures. Briefly, astrocytes were trypsinized and replated onto poly-D-lysine/laminin-coated coverslips. Transfection was done using the Neon transfection kit (MPK1096; Invitrogen, Carlsbad, CA). All the experiments were performed at least three times from independent cells/cultures, and ~100 cells were counted per experiment.

Scratch-induced migration and polarization assays

Astrocytes were seeded onto poly-D-lysine/laminin-coated 12-well plates and were grown to confluence in serum-containing medium, which was changed 1d prior to the scratch. Individual wounds were made with a P1000 tip, and wound closure occurred ~48–50 h later. Polarized microtubule protrusion was assessed using Zeiss Apotome epifluorescence microscopy (Jena, Germany). Cells were fixed and stained 18 h postscratch with an α-acetylated tubulin antibody. Centrosome reorientation was determined as previously described (Etienne-Manneville, 2006). In brief, 18 h after wounding, the astrocytes were fixed and stained with α-pericentrin antibodies (to mark centrosomes) and Hoechst (to mark nuclei). Cells in which

also blotted with α-GAPDH antibodies for a loading control. (K) Quantification of PKCζ levels from (J). $N = 3$. (L) Bcr reduces PKCζ levels in a Rac-dependent manner. Western blot analysis of lysates obtained from WT and *Bcr*$^{-/-}$ cortical mouse astrocytes treated overnight with PBS (control) or 50 µM of the Tiam1/Rac inhibitor NSC23766. Lysates were blotted with α-GAPDH for a loading control. (M) Quantification of PKCζ levels from (L). $N = 3$. Data are shown ± SEM.

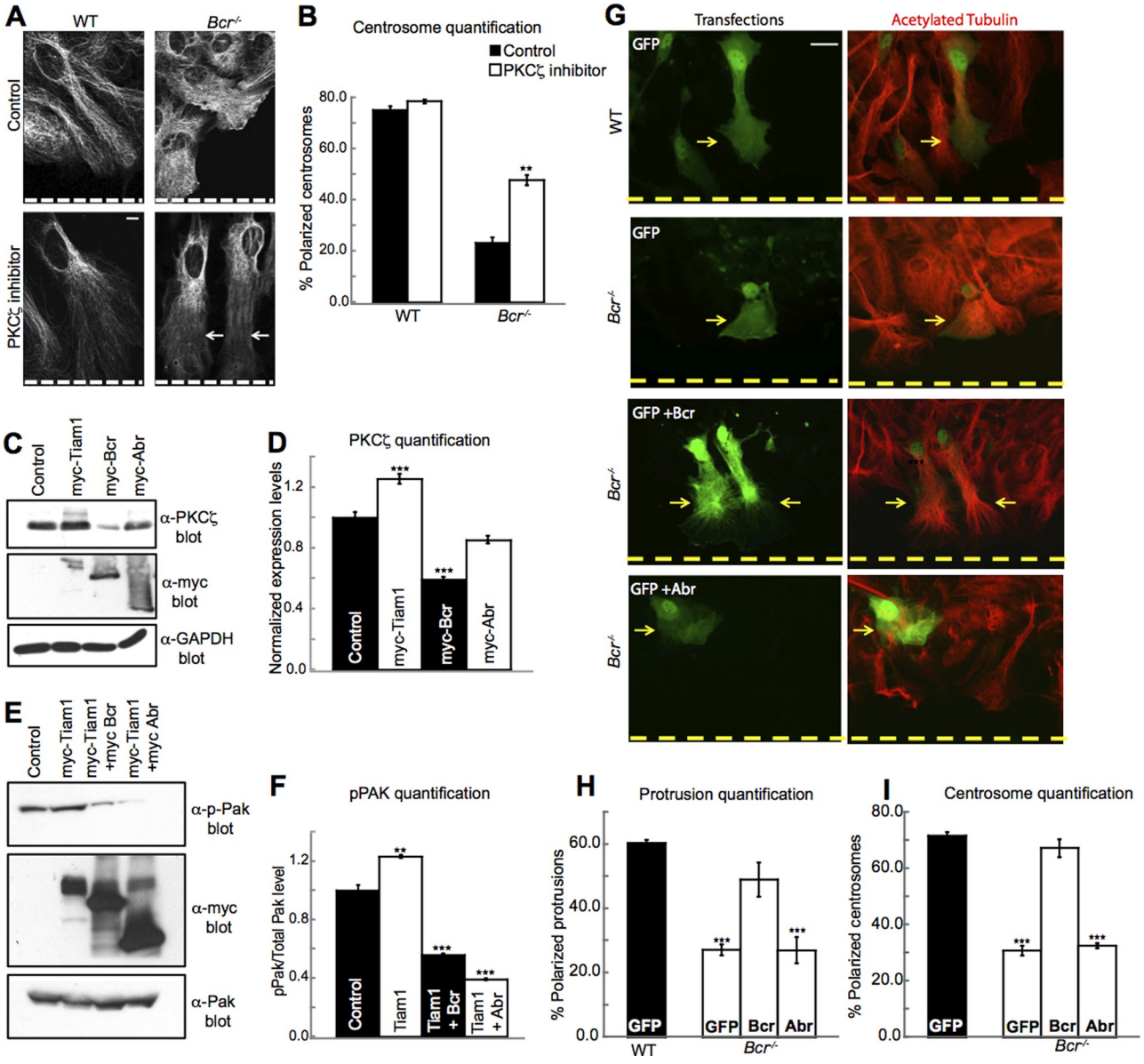

FIGURE 5: Bcr regulates polarity by restricting PKCζ function. (A) PKCζ inhibitor can partially rescue protrusion formation in *Bcr*$^{-/-}$ cortical mouse astrocytes. Representative images showing WT and *Bcr*$^{-/-}$ astrocytes treated overnight with PBS (control) or 10 μM of PKCζ pseudosubstrate inhibitor and then fixed and immunostained for acetylated tubulin. Dashed white line represents the scratch. Scale bar: 10 μm. n = ~100; N = 3. (B) PKCζ inhibitor can partially rescue centrosome reorientation in *Bcr*$^{-/-}$ cortical mouse astrocytes. Quantification of polarized centrosomes in WT and *Bcr*$^{-/-}$ cortical mouse astrocytes treated overnight with PBS (control) or 10 μM of PKCζ pseudosubstrate inhibitor. n = ~100; N = 3. (C) Overexpression of Bcr, but not Abr, negatively regulates PKCζ levels. Western blot analysis was performed on lysates from COS7 cells expressing control (empty vector) or myc-tagged Tiam1, Bcr, or Abr. Lysates were immunoblotted with α-PKCζ antibodies to assess PKCζ levels and α-GAPDH for a loading control. N = 3. (D) Quantification of PKCζ levels from (C). N = 3. (E) Bcr and Abr overexpression reduces Pak phosphorylation in COS7 cells. Western blot analysis of lysates from COS7 cells expressing control (myc) or myc-tagged Tiam1, Tiam1 and Bcr, or Tiam1 and Abr, immunoblotted for PKCζ. Lysates were blotted with an α-GAPDH antibody for a loading control. (F) Quantification of PKCζ levels from (E). N = 3. (G) Expression of Bcr, but not Abr, rescues protrusion defects in *Bcr*$^{-/-}$ cortical mouse astrocytes. WT astrocytes were transfected with eGFP as a positive control. *Bcr*$^{-/-}$ astrocytes were transfected with eGFP alone or in combination with Bcr or Abr expression plasmids, and then astrocytes were subjected to scratch assays. Cells were then fixed 18 h postscratch and immunostained for acetylated tubulin (red). Yellow dashed line represents scratch. Scale bar: 10 μm. (H) Quantification of the protrusion assay. n = ~100; N = 3. (I) Expression of Bcr, but not Abr, can rescue centrosome reorientation defects in *Bcr*$^{-/-}$ cortical mouse astrocytes. Quantification of polarized centrosomes in WT astrocytes transfected with eGFP (positive control) or *Bcr*$^{-/-}$ cortical mouse astrocytes transfected with eGFP, eGFP and Bcr, or eGFP and Abr. n = ~100; N = 3. Data are shown ± SEM.

the centrosome was within a quadrant whose angular bisector was perpendicular to the wound were scored as polarized centrosomes. Centrosome reorientation studies were imaged using Zeiss Apotome epifluorescence microscopy, and colocalization studies were imaged using a Leica TCS SP2 confocal microscope. All the experiments were done at least three times from independent cultures, and ~100 cells were counted per experiment.

Scratch assay and random migration movies

Live imaging was carried out with an Olympus IX81 inverted microscope with a Retiga camera (QImaging) and a live-cell environmental chamber (PrecisionControl). Cells were plated to confluence on coated 24-well glass tissue plates (Greiner Bio-One) and scratched vertically. Images were taken at 100× every 30 min over a 48-h period. Movies were then compiled from these snapshots in SlideBook. For tracing experiments, cells were plated at low confluence on coated glass plates (Greiner Bio-One) and imaged over 24 h at 30-min intervals. These data were used to calculate the total displacement and end point displacement of each point. The nuclei of five cells/well were manually tracked across 30 frames. All the experiments were done in triplicate and were repeated at least three times from independent cultures.

Antibodies and drugs

The following antibodies are commercially available: α-Bcr (N-20/C-20), α-Tiam1 (C-16), α-Myc (9E10), and α-PKCζ (C-20) (Santa Cruz Biotechnology, Santa Cruz, CA); α-Rac1, α-Cdc42, α-Pak, and α-p-GSK3β (Ser-9) (Cell Signaling Technology, Danvers, MA); α-Abr, α-GSK3β (BD Biosciences, Franklin Lakes, NJ); α-Flag M2, α-GFAP, and α-acetylated tubulin (Sigma-Aldrich, St. Louis, MO); α-GAPDH and α-Par3 (Millipore, Billerica, MA); α-pericentrin (Covance, Princeton, NJ). α-P-Pak was previously described (Tolias *et al.*, 2005, 2007). Alexa Texas Red Phalloidin was purchased from Invitrogen. NSC23766 was purchased from Tocris Biosciences. PKCζ pseudosubstrate inhibitor was from Santa Cruz Biotechnology. GM132 was purchased from EMD4Biosciences. Cell proliferation was measured using the BrdU kit from Millipore.

Immunohistochemistry

Cells were fixed for 15 min at room temperature in 4% paraformaldehyde in phosphate-buffered saline (PBS) or in ice-cold methanol for 15 min (pericentrin staining). Cells were permeabilized in 0.3% Triton X-100, 15% goat serum, and 5% bovine serum albumin in PBS for 1 h at room temperature and then immunostained with primary antibodies overnight at 4°C. Cy3- and Cy5-conjugated secondary antibodies (Jackson ImmunoResearch, West Grove, PA) were used at 1:500 dilutions for double immunolabeling. All the experiments were done at least three times from independent cultures, and ~100 cells were counted per experiment.

Immunoprecipitation and Western blot analysis

Cultured rat astrocytes and transfected COS7 cells were lysed in buffer containing 50 mM Tris (pH 7.5), 150 mM NaCl, 1 mM EDTA, 1% Nonidet P-40, 10% glycerol, 1 mM dithiothreitol (DTT), 1 mM Na_3VO_4, 10 mM NaF, 10 mM β- glycerol phosphate, and protease inhibitors (Roche, Indianapolis, IN). Cell lysates were centrifuged 10–15 min at 14,000 rpm at 4°C, and the postnuclear supernatant was incubated with 1 μg primary antibodies for 90 min at 4°C; this was followed by a 90-min incubation with protein A or G agarose beads (Roche). Precipitates were washed four times, and bound proteins were eluted with SDS–PAGE sample buffer. The samples were separated on 8% polyacrylamide gels, transferred to polyvinylidene fluoride membranes, and blocked with 5% nonfat dry milk in Tris buffer saline (TBS) containing 0.1% Tween-20. Blots were then incubated with primary antibodies at 4°C overnight and then with horseradish peroxidase–conjugated secondary antibodies (Calbiochem, San Diego, CA) for 1 h at 25°C. Signals were visualized using enhanced chemiluminescence. All the experiments were done at least three times from independent cultures.

Rac1/Cdc42 activation assay

Cortical astrocytes were harvested in Mg^{2+} lysis buffer containing 25 mM HEPES (pH 7.5), 150 mM NaCl, 1% Nonidet P-40, and 10 mM $MgCl_2$, supplemented with 1 mM DTT, 1 mM Na_3VO_4, 10 mM NaF, 10 mM β-glycerol phosphate, and protease inhibitors (Roche). The lysates were incubated with a GST-PAK1-PBD fusion protein immobilized on glutathione agarose beads for 20 min at 4°C. Following precipitation, the pellets were washed three times with Mg^{2+} lysis buffer and then analyzed by Western blotting with α-Rac1 or α-Cdc42 antibodies to determine the levels of active Rac1 or Cdc42, respectively. All the experiments were done at least three times from independent cultures.

Statistical analysis

Statistical analyses were performed with KaleidaGraph. Statistical significance was calculated using Student's *t* test for comparison between two independent groups and analysis of variance with Tukey's post hoc test for multiple-group comparisons. Error bars represent SEM. Statistical significances were determined at *, $p < 0.05$; **, $p < 0.001$; and ***, $p < 0.0001$.

ACKNOWLEDGMENTS

We thank N. Heisterkemp for generously providing $Abr^{-/-}$ mice and Abr cDNA constructs and A. Toker for providing PKCζ reagents. We thank A. Sokac, M. Rasband, and J. Duman for critical reading of the manuscript; J. Duman, S. Mulherkar, and other Tolias lab members for technical advice, critical discussions, and reagents; F. Liu and K. Firozi for administrative support and animal handling; L. Zheng for technical help; and T. Vadakkan for help with image analysis. This work was supported by National Institutes of Health grant R01NS062829 (to K.F.T.), Department of Defense Grant W81XWH-08-2-0148 (to K.F.T), and the Mission Connect/TIRR Foundation.

REFERENCES

Aranda V, Nolan ME, Muthuswamy SK (2008). Par complex in cancer: a regulator of normal cell polarity joins the dark side. Oncogene 27, 6878–6887.

Cau J, Hall A (2005). Cdc42 controls the polarity of the actin and microtubule cytoskeletons through two distinct signal transduction pathways. J Cell Sci 118, 2579–2587.

Chan JR, Jolicoeur C, Yamauchi J, Elliott J, Fawcett JP, Ng BK, Cayouette M (2006). The polarity protein Par-3 directly interacts with p75NTR to regulate myelination. Science 314, 832–836.

Chen X, Macara IG (2005). Par-3 controls tight junction assembly through the Rac exchange factor Tiam1. Nat Cell Biol 7, 262–269.

Cho YJ, Cunnick JM, Yi SJ, Kaartinen V, Groffen J, Heisterkamp N (2007). Abr and Bcr, two homologous Rac GTPase-activating proteins, control multiple cellular functions of murine macrophages. Mol Cell Biol 27, 899–911.

Cunliffe HE, Jiang Y, Fornace KM, Yang F, Meltzer PS (2012). PAR6B is required for tight junction formation and activated PKCζ localization in breast cancer. Am J Cancer Res 2, 478–491.

Eder AM *et al.* (2005). Atypical PKCι contributes to poor prognosis through loss of apical-basal polarity and cyclin E overexpression in ovarian cancer. Proc Natl Acad Sci USA 102, 12519–12524.

Ellenbroek SI, Iden S, Collard JG (2012a). Cell polarity proteins and cancer. Semin Cancer Biol 22, 208–215.

Ellenbroek SI, Iden S, Collard JG (2012b). The Rac activator Tiam1 is required for polarized protrusional outgrowth of primary astrocytes by affecting the organization of the microtubule network. Small GTPases 3, 4–14.
Etienne-Manneville S (2004). Cdc42—the centre of polarity. J Cell Sci 117, 1291–1300.
Etienne-Manneville S (2006). In vitro assay of primary astrocyte migration as a tool to study Rho GTPase function in cell polarization. Methods Enzymol 406, 565–578.
Etienne-Manneville S (2008). Polarity proteins in glial cell functions. Curr Opin Neurobiol 18, 488–494.
Etienne-Manneville S, Hall A (2001). Integrin-mediated activation of Cdc42 controls cell polarity in migrating astrocytes through PKCζ. Cell 106, 489–498.
Etienne-Manneville S, Hall A (2002). Rho GTPases in cell biology. Nature 420, 629–635.
Etienne-Manneville S, Hall A (2003a). Cdc42 regulates GSK-3β and adenomatous polyposis coli to control cell polarity. Nature 421, 753–756.
Etienne-Manneville S, Hall A (2003b). Cell polarity: Par6, aPKC and cytoskeletal crosstalk. Curr Opin Cell Biol 15, 67–72.
Gao Y, Dickerson JB, Guo F, Zheng J, Zheng Y (2004). Rational design and characterization of a Rac GTPase-specific small molecule inhibitor. Proc Natl Acad Sci USA 101, 7618–7623.
Gardiner EM, Pestonjamasp KN, Bohl BP, Chamberlain C, Hahn KM, Bokoch GM (2002). Spatial and temporal analysis of Rac activation during live neutrophil chemotaxis. Curr Biol 12, 2029–2034.
Gomes ER, Jani S, Gundersen GG (2005). Nuclear movement regulated by Cdc42, MRCK, myosin, and actin flow establishes MTOC polarization in migrating cells. Cell 121, 451–463.
Groffen J, Heisterkamp N (1997). The chimeric BCR-ABL gene. Baillieres Clin Haematol 10, 187–201.
Hooshmand-Rad R, Claesson-Welsh L, Wennstrom S, Yokote K, Siegbahn A, Heldin CH (1997). Involvement of phosphatidylinositide 3′-kinase and Rac in platelet-derived growth factor-induced actin reorganization and chemotaxis. Exp Cell Res 234, 434–441.
Iden S, Collard JG (2008). Crosstalk between small GTPases and polarity proteins in cell polarization. Nat Rev Mol Cell Biol 9, 846–859.
Kraynov VS, Chamberlain C, Bokoch GM, Schwartz MA, Slabaugh S, Hahn KM (2000). Localized Rac activation dynamics visualized in living cells. Science 290, 333–337.
Li L, Yuan H, Weaver CD, Mao J, Farr GH, III, Sussman DJ, Jonkers J, Kimelman D, Wu D (1999). Axin and Frat1 interact with dvl and GSK, bridging Dvl to GSK in Wnt-mediated regulation of LEF-1. EMBO J 18, 4233–4240.
Mardilovich K, Olson MF, Baugh M (2012). Targeting Rho GTPase signaling for cancer therapy. Future Oncol 8, 165–177.
Mertens AE, Pegtel DM, Collard JG (2006). Tiam1 takes PARt in cell polarity. Trends in Cell Biol 16, 308–316.
Moon RT, Bowerman B, Boutros M, Perrimon N (2002). The promise and perils of Wnt signaling through β-catenin. Science 296, 1644–1646.
Nakayama M, Goto TM, Sugimoto M, Nishimura T, Shinagawa T, Ohno S, Amano M, Kaibuchi K (2008). Rho-kinase phosphorylates PAR-3 and disrupts PAR complex formation. Dev Cell 14, 205–215.
Nishimura T, Yamaguchi T, Kato K, Yoshizawa M, Nabeshima Y, Ohno S, Hoshino M, Kaibuchi K (2005). PAR-6-PAR-3 mediates Cdc42-induced Rac activation through the Rac GEFs STEF/Tiam1. Nat Cell Biol 7, 270–277.
Pegtel DM, Ellenbroek SI, Mertens AE, van der Kammen RA, de Rooij J, Collard JG (2007). The Par-Tiam1 complex controls persistent migration by stabilizing microtubule-dependent front-rear polarity. Curr Biol 17, 1623–1634.
Qiu RG, Abo A, Steven Martin G (2000). A human homolog of the *C. elegans* polarity determinant Par-6 links Rac and Cdc42 to PKCζ signaling and cell transformation. Curr Biol 10, 697–707.
Rathinam R, Berrier A, Alahari SK (2011). Role of Rho GTPases and their regulators in cancer progression. Front Biosci (Landmark Ed) 16, 2561–2571.
Regala RP, Weems C, Jamieson L, Copland JA, Thompson EA, Fields AP (2005a). Atypical protein kinase Cι plays a critical role in human lung cancer cell growth and tumorigenicity. J Biol Chem 280, 31109–31115.
Regala RP, Weems C, Jamieson L, Khoor A, Edell ES, Lohse CM, Fields AP (2005b). Atypical protein kinase Cι is an oncogene in human non-small cell lung cancer. Cancer Res 65, 8905–8911.
Ridley AJ (2001). Rho GTPases and cell migration. J Cell Sci 114, 2713–2722.
Ruiz-Canada C, Ashley J, Moeckel-Cole S, Drier E, Yin J, Budnik V (2004). New synaptic bouton formation is disrupted by misregulation of microtubule stability in aPKC mutants. Neuron 42, 567–580.
Sander EE, van Delft S, ten Klooster JP, Reid T, van der Kammen RA, Michiels F, Collard JG (1998). Matrix-dependent Tiam1/Rac signaling in epithelial cells promotes either cell-cell adhesion or cell migration and is regulated by phosphatidylinositol 3-kinase. J Cell Biol 143, 1385–1398.
Schmidt A, Hall A (2002). Guanine nucleotide exchange factors for Rho GTPases: turning on the switch. Genes Dev 16, 1587–1609.
Shi SH, Cheng T, Jan LY, Jan YN (2004). APC and GSK-3β are involved in mPar3 targeting to the nascent axon and establishment of neuronal polarity. Curr Biol 14, 2025–2032.
Smith L, Chen L, Reyland ME, DeVries TA, Talanian RV, Omura S, Smith JB (2000). Activation of atypical protein kinase C ζ by caspase processing and degradation by the ubiquitin-proteasome system. J Biol Chem 275, 40620–40627.
Solecki DJ, Govek EE, Hatten ME (2006). mPar6α controls neuronal migration. J Neurosci 26, 10624–10625.
Tcherkezian J, Lamarche-Vane N (2007). Current knowledge of the large RhoGAP family of proteins. Biol Cell 99, 67–86.
Tolias KF, Bikoff JB, Burette A, Paradis S, Harrar D, Tavazoie S, Weinberg RJ, Greenberg ME (2005). The Rac1-GEF Tiam1 couples the NMDA receptor to the activity-dependent development of dendritic arbors and spines. Neuron 45, 525–538.
Tolias KF, Bikoff JB, Kane CG, Tolias CS, Hu L, Greenberg ME (2007). The Rac1 guanine nucleotide exchange factor Tiam1 mediates EphB receptor-dependent dendritic spine development. Proc Nat Acad Sci USA 104, 7265–7270.
Wolf AM, Lyuksyutova AI, Fenstermaker AG, Shafer B, Lo CG, Zou Y (2008). Phosphatidylinositol-3-kinase-atypical protein kinase C signaling is required for Wnt attraction and anterior-posterior axon guidance. J Neurosci 28, 3456–3467.
Zhang H, Macara IG (2006). The polarity protein PAR-3 and TIAM1 cooperate in dendritic spine morphogenesis. Nat Cell Biol 8, 227–237.
Zhang H, Macara IG (2008). The PAR-6 polarity protein regulates dendritic spine morphogenesis through p190 RhoGAP and the Rho GTPase. Dev Cell 14, 216–226.